Available online at www.sciencedirect.com
SCIENCE DIRECT®

Journal of the European Ceramic Society 24 (2004) 3345–3350

www.elsevier.com/locate/jeurceramsoc

Mechanical properties of Si_3N_4/SiC nanocomposites studied by instrumented indentation with spheres

P. Hvizdoš[a], M. Kašiarová[a], J. Dusza[a], Miroslav Hnatko[b], Pavol Šajgalík[b,*]

[a]*Institute of Materials Research, Slovak Academy of Sciences, Košice, Slovakia*
[b]*Institute of Inorganic Chemistry, Slovak Academy of Sciences, Dubravska cesta 9, Bratislava 842 36, Slovakia*

Abstract

Contact deformation behaviour and mechanical properties of two Si_3N_4/SiC nanocomposites with different SiC content were investigated by nanoindentation with spherical diamond indenter (radius 5 μm) at low loads (1–300 mN) using depth sensing techniques. From the measurement of the tip displacement depending on the load and the tip geometry, the total and the remnant depth of penetration were found. Based on the results we were able to study elastic, yield and plastic behaviour. Using the method of partial unloading, the contact stress-strain curves, hardness, and modulus of elasticity were explored. The results were compared to the values obtained by the same method for the reference Si_3N_4 material.

Keywords: Nanocomposites; Mechanical properties; Si_3N_4; SiC; Spherical indenters

1. Introduction

Recently, there has been a great world-wide interest in developing and characterizing new nano-structured materials. These newly developed materials are often prepared in limited quantities and shapes unsuitable for extensive mechanical testing. The development of depth sensing indentation methods have introduced the advantage of load and depth measurement during the indentation cycle. This enables, using simple and fast measurement, to evaluate not only hardness, for which the indentation is traditionally used, but also elastic properties, as well as time dependent phenomena such as creep and recovery and the energy absorbed during indentation. Furthermore, when spherical rather then pointed indenters are used, it is possible to investigate also elastic-to-plastic transition, yield, as well as the onset of other irreversible deformation processes such as cracking or pressure induced phase transformations.[1] These problems can be studied on very small samples, with high spatial resolution, and non-destructively, if necessary. A comparative study of instrumented indentation with spherical and pyramidal indenters with traditional Vickers indentation was published in our previous work.[2]

Since Niihara published his seminal work on ceramic nanocomposites[3] various ways of production such materials have been used:[4,5] mechanical mixing of submicron crystalline SiC and Si_3N_4 powders, CVD, using plasma-chemically or polymer derived amorphous starting powder of Si–C–N type as precursors to SiC particles formation. Šajgalík et al.[6] recently developed a cost-effective method in which Si–C–N amorphous powder is substituted by a cheaper mixture of silica and carbon black. In this method, the SiC nanoparticles are formed during sintering by carbothermic reduction of SiO_2 by elemental C. The motivation for the present work was the quality assessment of the obtained material by comparison with another, compositionally analogous, nanocomposite prepared by a different, more traditional, way. The main aim was then to investigate some basic mechanical properties of two newly developed nanocomposites using depth-sensing indentation and to relate them to the reference monolithic silicon nitride.

2. Theoretical background: indentation with spheres

Indentation of an infinite half space by a sphere is initially elastic and was first considered by Hertz,[7] who suggested that the critical transition force for the onset

* Corresponding author. Tel.: +421-7-594-10-400; fax: 421-7-594-10-444.
E-mail address: usahsajg@savba.sk (P. Šajgalík).

0955-2219/$ - see front matter © 2003 Elsevier Ltd. All rights reserved.
doi:10.1016/j.jeurceramsoc.2003.10.028

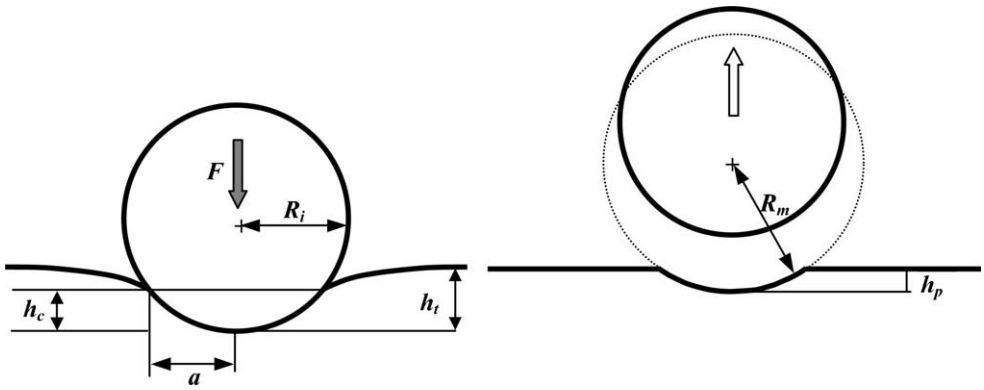

Fig. 1. Schematic illustration of indentation of flat surface by spherical indenter.

of plastic deformation then can be used for material characterization. The elastic penetration, h_e, of a sphere (indenter) of radius R_i into a flat surface (tested material) under force F is given[8]

$$h_e = (9/16)^{1/3}(F/E^*)^{2/3}(1/\mathrm{Ri})^{1/3}. \quad (1)$$

Here E^* is the composed (indenter/material) elastic modulus

$$1/E^* = \left(1-\upsilon_m^2\right)/E_m + \left(1-\upsilon_i^2\right)/E_i, \quad (2)$$

where ν_m and E_m are Poisson's ratio and elastic modulus of the material, ν_i and E_i are Poisson's ratio and elastic modulus of the indenter.

The mean pressure ($P_m = F/A$, where A is the area of contact) over the elastic footprint increases with the loading force until it reaches a limiting value set by yield stress of the undeformed material. From this point on any increase in the load is accompanied by plastic yielding to limit the mean pressure to a value consistent with the yield stress of the deforming material. A plastic zone forms beneath the indenter and after unloading a residual impression is left in the surface. The total depth of penetration (h_t) is then a sum of the elastic (h_e) and plastic (h_p) components, as it is illustrated also in Figs. 1 and 2:

$$h_t = h_e + h_p. \quad (3)$$

Assuming that the elastic deformation is equally distributed above and below the circle of contact, the depth of penetration in contact (h_c), which also contains plastic and elastic components, is given as[1]

$$h_c = h_t - h_e/2. \quad (4)$$

The radius of circle of contact (a) is then given by geometry as

$$a^2 = 2R_i h_c - h_c^2. \quad (5)$$

Because unloading in quasi-static regime is entirely elastic, the unloading curve can be analysed using Hertzian elastic contact mechanics and the Eq. (1) becomes

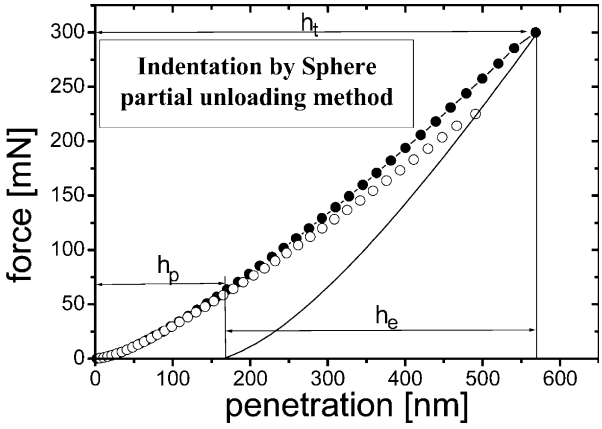

Fig. 2. Example of force-penetration data (SNSC nanocomposite) from multiple partial unloading method (fully loaded (●) and partially unloaded (○) points), illustrating separation of elastic and plastic parts from total depth of penetration.

$$h_e = (9/16)^{1/3}(F/E^*)^{2/3}(1/R_i - 1/R_m)^{1/3}, \quad (6)$$

where R_m is the curvature radius of the residual spherical depression, which can be found as

$$R_m = \left(a^2 + h_p^2\right)/2h_p. \quad (7)$$

The elastic modulus can be calculated directly from the unloading curve.

The critical stress condition, where transition from elastic to elastic/plastic behaviour occurs, exists when the mean pressure equals the hardness of the tested surface. Therefore, at loads above the critical value, the hardness can be calculated as

$$H = F/\pi a^2. \quad (8)$$

3. Experimental material

The investigation was carried out on two nanocomposites prepared by different processing routes which, however, were to yield similar final compositions–silicon

Table 1
Compositions of the starting powder mixtures

Material	Si_3N_4 (wt.%)	Y_2O_3 (wt.%)	SiO_2 (wt.%)	C (wt.%)	SiC (wt.%)
SNYC2B	84.12	4.43	7.39	4.05	–
SNSC	90.25	4.75	–	–	5

nitride matrix with ~5% of SiC nanoparticles. The experimental materials were prepared in the Institute of Inorganic Chemistry in Bratislava. The starting compositions of the studied materials are given in Table 1.

The SNYC2B was prepared by adding carbon black and SiO_2 into the starting mixture. The SNSC material was prepared by direct adding of SiC nanoparticles into the $Si_3N_4 + Y_2O_3$ powder mixture.

In both cases the starting powder mixtures were homogenized by attrition in a polyethylene bottle with Si_3N_4 spheres in isopropanol for 24 h. Subsequently, the dried mixtures were sieved through 25 μm sieve in order to eliminate the large agglomerates. Green discs with the diameter of 48 and 8 mm thick were die pressed. Then they were embedded into a BN powder bed and hot-pressed in nitrogen atmosphere under pressure of 30 MPa at 1750 °C for 2 h. The desired SiC nanoparticles in the SNYC2B were formed during sintering by carbothermic reduction.[6]

The reference silicon nitride was a commercial material SL200 fabricated by CeramTech, Plochingen, Germany, which was recently an object of extensive study in the European Structural Integrity Society's (ESIS) testing program for a silicon nitride reference material.[9] It is a gas pressure sintered silicon nitride with additives Al_2O_3 (3 wt.%) and Y_2O_3 (3 wt.%). The material was provided by the manufacturer in form plates with dimensions of 47×11×102 mm.

For the indentation studies pieces of all materials with dimensions of 3×4×4 mm^3 were used. Their surfaces were polished to the 0.25 μm final finish.

4. Experimental methods

The nanoindentation tests, using the depth sensing technique (DST), were carried out on UMIS 2000 (made by CSIRO Australia) ultramicroindentation system at room temperature in ambient air.

In the case of the spherical indenter the multiple partial unloading method, developed by Field and Swain[10,11] and recently studied in detail by Bushby,[1] was used. In this method a single indentation is partially unloaded at each force step by a specific fraction (from 10 to 90%) of the load step. Each force step then provides two pieces of information: the total depth of elastic/plastic penetration and a measure of the recovery from that load.

When the unloading part of the load cycle can be completely modelled analytically, such as the case of indentation with sphere, two points at each load are sufficient to fully characterise unloading from each loading step. The residual unrecovered indentation depth (h_p), the elastic deflection of surface (h_e), the depth below the circle of contact (h_c) were then calculated for each load step.

In the present study the spherical diamond indenter with nominal radius $R_i = 5$ μm was used. Its modulus of elasticity was 1150 GPa and the Poisson's ratio 0.07. Loading force up to 300 mN in 30 incremental steps was applied, each step was followed by 25% unloading. On each specimen at least 20 tests were perfomed, randomly distributed on the polished surfaces.

The modulus of elasticity of the material was calculated using Eq. (6) for each step's penetration depth, assuming $\nu_m = 0.2$ (value for Si_3N_4).[12] The hardness was calculated from Eq. (8) at loads from 270 to 300 mN which induced stresses well above the transition point. The partial unloading procedure also allows an indentation stress-strain curves to be generated, where the mean pressure (P_m) is taken as indentation stress, and indentation strain is expressed as the ratio of a/R_i.

5. Results and discussion

Microstructures of the studied materials were described in details in[9,13–15] The SiC nanoparticles were localized both inside the matrix gains and along grain boundaries in the intergranular glassy phase. Their presence hinders the Si_3N_4 grain growth and results in finer microstrucure of the nanocomposites. Average matrix grain size was 150–200 nm for the SNSC, 150–180 nm for the SNYC2B, while that for the monolithic Si_3N_4 was ~790 nm.

Fig. 2 shows typical result (SNSC composite) of one partial unloading test in form of the force-penetration data for extreme points at each step. When the material deforms elastically, the data for fully loaded and partially unloaded states lie on the same line. After exceeding the yielding point of the material, the recovery is not longer complete and two branches diverge. Each particular data pair lies on a curve equivalent to single loading-unloading, and allows to find elastic and plastic portion of penetration for each particular load, as it is

Table 2
Mechanical properties measured by nanoindentation

Material	Young's modulus (GPa)	Hardness (GPa)	Yielding point (GPa)
SNYC2B	320.2±4.6	28.3±0.3	17.06±0.87
SNSC	304.2±14.9	23.2±0.8	14.70±1.36
Si_3N_4	313.0±3.8	23.7±0.5	14.44±0.58

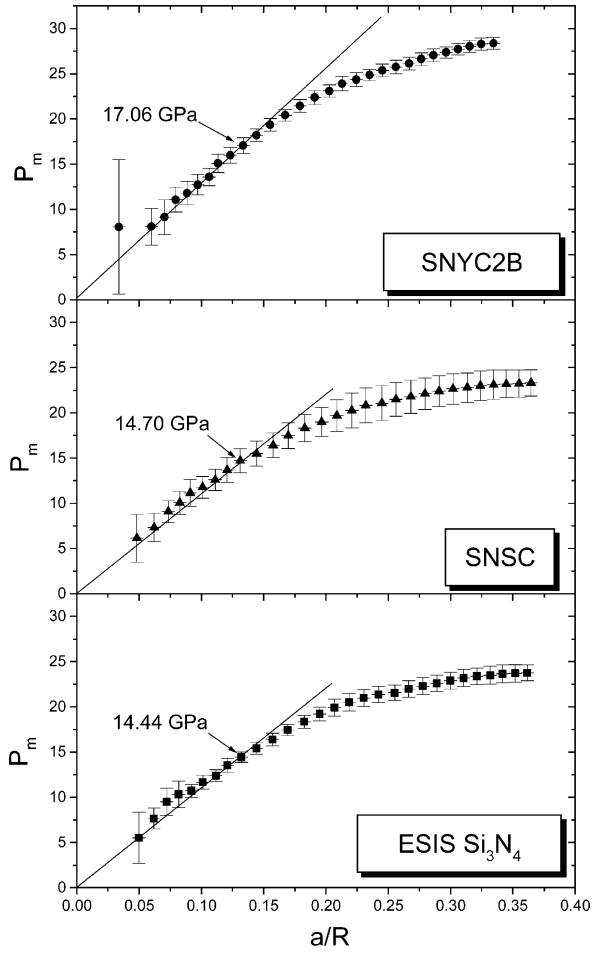

Fig. 3. Indentation stress–strain curves in the mean pressure (P_m) vs normalized contract radius (a/R) representation for all studied materials. The straight lines illustrate the initial elastic portion of indentation and the arrows mark the yielding points.

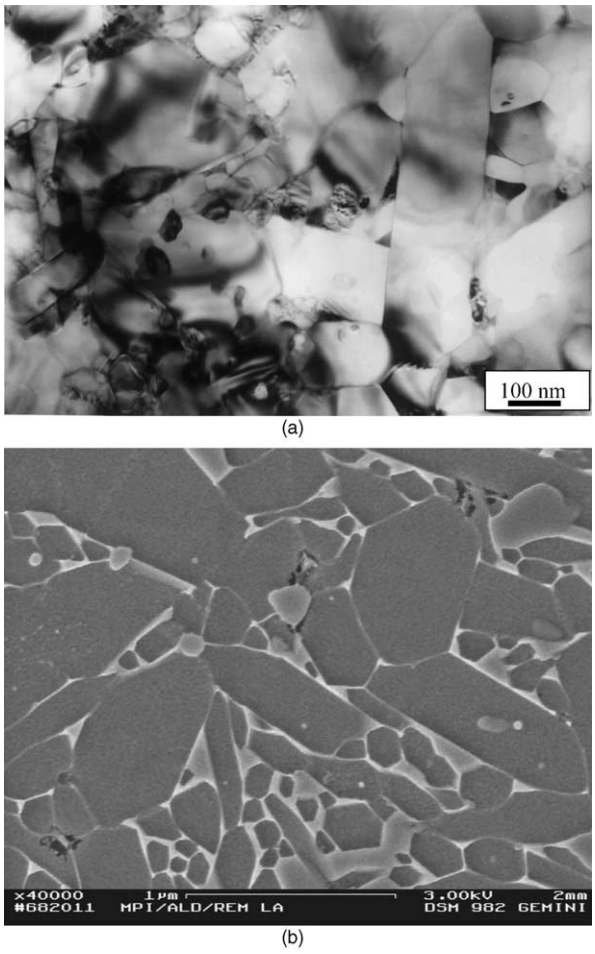

Fig. 4. (a) Microstructure of the SNSC composite showing a cluster of intergranular SiC grains. Area to the left contains numerous SiC inclusions, whereas to the right their content is much lower. (b) Arrays of microvoids around the SiC particles and between the matrix grains in the SNSC composite.

illustrated in the Fig. 2 for the maximum load by the solid line.

The results of the measurements are summarized in Table 2. The Young's modulus of the reference monolithic material agrees within the scatter very well with literature data (310 GPa in[16]). The value for the composite can be estimated using the law of mixtures, $E = E_a V_a + E_b V_b$, where V_a and V_b are the volume fractions of the constituents. For our materials containing 5% of SiC with modulus of elasticity 440 GPa[16] this law gives $E = 316.5$ GPa. This is in an excellent agreement with the value for the SNYC2B (320.2±4.6 GPa). The other nanocomposite exhibited comparably lower value but much higher scatter, which suggests that on some places of the tested surface the influence of the SiC grains was much stronger than on others.

The hardness values generally seem to be a little overestimated. This can be partly due to the size of the stress field. The sizes of contact areas and also the stress fields dimensions at relatively low loads used in our tests were typically in range of 0.1 to 2 μm, that is the values comparable with the size of single matrix grain or a few nanosized grains, which means that the influence of the porosity was negligible. The hardness of SNSC and Si_3N_4 corresponds very well to the hardness data[12] for

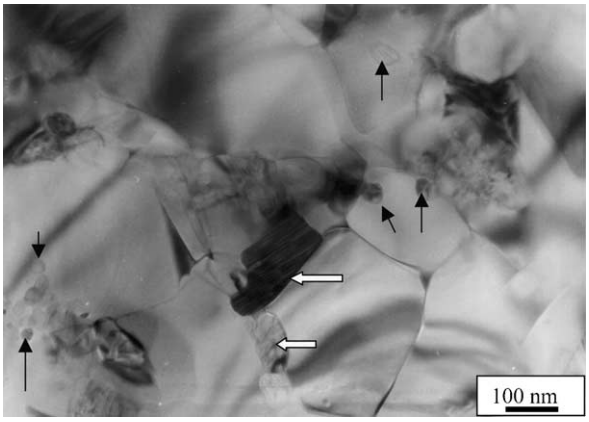

Fig. 5. Microstructure of the SNYC2B. The white arrows point to a couple of intergranular SiC particles, the black arrows show some of many intragranular globular nanoparticles, integrated inside the silicon nitride grains.

pure high density HPSN (22 GPa). In the SNYC2B the influence of SiC (hardness 27–33 GPa) is significant.

Fig. 3 shows the indentation stress-strain curves for all studied materials obtained from the force-penetration data. At the very low loads, the readings are accompanied by considerable errors due to relatively large scatter in measurement of penetration depth which is frequently less than 20 nm and thus close to the instrument resolution limits. However, at higher loads the linear initial portion corresponding to purely elastic deformation can be identified. Yielding point then can be found as the deviation from this elastic behaviour. The obtained values are introduced in Table 2. It is difficult to relate them to other results due to the lack of such data in literature, but they are similar to the onset of plastic deformation for pure polycrystalline alumina (~14 GPa).[1] Such information for ceramics and glasses is unique because conventional tensile or compressive tests normally result in catastrophic failure at much lower stresses.

General tendency to higher scatter of mechanical properties in the SNSC nanocomposite, as it can be seen in Fig. 3 over the whole load interval, and also in Table 2, suggests that mechanical homogenization of Si_3N_4 grains and SiC nanopowder produced less regular microstructure than was that of SNYC2B. The average values were usually close to that of the monolithic Si_3N_4 which means that in most cases only Si_3N_4 grains were probed.

In order to clarify these findings, microstructure features of both nanocomposites were investigated on submicron scale using transmission electron microscopy of thin foils and scanning electron microscopy of plasma etched surfaces with main focus on the size, shape, and distribution of SiC nanoparticles. These studies showed that in both cases the microstructures were characterized by submicron matrix grains with occasional occurrence of larger rod-like β-Si_3N_4 crystals. Both SNYC2B and SNSC contained SiC nanoparticles placed inter- and intra-granularly, randomly distributed in microstructure. The intergranular particles were more frequent in SNSC, they had size usually about 100 nm, had irregular elongated shape and often contained systems of stacking faults. They reinforced the grain boundaries but tended to form clusters (Fig. 4a). Another feature observed in the SNSC were arrays of microvoids and micropores, also showed in Fig. 4b. Morphologically, the intragranular particles were similar to the intergranular ones in this material. In the SNYC2B the particles were located mostly inside the Si_3N_4 grains, they were usually almost globular and smaller than 50 nm (Fig. 5). They were dispersed in the microstructure more regularly.

According to these observations, occasional higher values of mechanical properties in the SNSC can be attributed to the influence of SiC grains integrated well inside the matrix grains, whereas the lower ones to the influence of microvoids and pores which remained in the microstructure. Among all tested materials the carbon-derived nanocomposite performed best in all tests.

6. Conclusions

The mechanical properties and deformation behaviour of two Si_3N_4/SiC nanocomposites and a reference monolithic silicon nitride were investigated by instrumented indentation. The method provided reliable results, which were in very good agreement with the literature data and enabled to investigate the elastic-to-elastic/plastic transition phenomena that are extremely difficult to study by using other methods.

The carbon-derived nanocomposite exhibited the best mechanical properties showing that introducing the SiC grains enhanced performance of the material and that the new cost-effective method of fabrication resulted in a suitable microstructure. The results of the nanocomposite with admixed SiC nanograins were similar to that of the monolithic material, however, they had the largest scatter which points to the less regular microstructure with respect to the SiC grains distribution.

Acknowledgements

The UMIS measurements were performed at Queen Mary University of London. The authors wish to thank to Dr. A J Bushby for his help with the nanoindentation experiments. The work was supported by NANOSMART, Centre of Excellence of SAS, and financed by the Slovak Grant Agency for Science via grant No. 2/1166/21.

References

1. Bushby, A. J., Nano-indentation using spherical indenters. *Non-destructive Testing and Evaluation*, 2001, **17**, 213–220.
2. Hvizdoš, P., Kašiarová, M., Dusza, J., Šajgalík, P. and Hnatko, M., Mechanical properties of Si_3N_4/SiC nanocomposite measured by nanoindentation. *Powder Metallurgy Progress*, 2003, **3**, 49–55.
3. Niihara, K., New design concept of structural ceramics—ceramic nanocomposites. *J. Jpn. Ceram. Soc.*, 1991, **99**, 974–982.
4. Rouxel, T., Wakai, F. and Izaki, K., Tensile ductility of superplastic Al_2O_3–Y_2O_3–Si_3N_4/SiC composites. *J. Am. Ceram. Soc.*, 1992, **75**, 2363–2372.
5. Herrmann, M., Schubert, C., Rendtel, A. and Hübner, H., Silicon nitride/silicon carbide nanocomposite materials: I. Fabrication and mechanical properties at room temperature. *J. Am. Ceram. Soc.*, 1998, **81**, 1095–1108.
6. Šajgalík, P., Hnatko, M., Lenčéš, Z., Warbichler, P. and Hofer, F., Carbon-derived Si_3N_4/SiC nanocomposite. *Zeitschrift für Metallkunde*, 2001, **92**, 937.
7. Hertz, H., *Miscellaneous Papers*. Macmillan, London, 1896.
8. Johnson, K. L., *Contact Mechnics*. Cambridge University Press, London, 1985.
9. Lube, T. Danzer, R., An ESIS testing program for a silicon nitride reference material. In *Proc. of the 14th European Conference of Fracture, Vol. II/III*, ed. A. Neimitz, I. V. Rokach, D. Kocanda and K. Golos, Kracov, Poland, 2002, pp. 401–408
10. Field, J. S. and Swain, M. V., A simple predictive model for spherical indentation. *J. Mater. Res.*, 1993, **8**, 297–306.
11. Field, J. S. and Swain, M. V., Determining the mechanical properties of small volumes of material from submicrometer spherical indentation. *J. Mater. Res.*, 1995, **10**, 101–112.
12. Richerson, D. W., *Modern Ceramic Engineering*. Marcel Dekker, New York, 1992.
13. Kovalčík, J., Dusza, J., Lube, T., Kübler, J. and Danzer, R., Slow crack growth behaviour of the ESIS silicon nitride material. In Proceedings of Deformation and Fracture in Structural PM Materials, ed. L. Parilák, and H. Danninger, Stará Lesná, Vol. 2, September 2002, pp. 71–75.
14. Kašiarová, M., Rudnayová, E., Kovalčík, J., Dusza, J., Hnatko, M., Šajgalík, P. and Merstallinger, A., Wear and creep characteristics of a carbon-derived Si_3N_4/SiC nanocomposite. *Mat.-wiss. u. Werkstofftech.*, 2003, **34**, 1–5.
15. Kašiarová, M., Hnatko, M., Dusza, J. and Šajgalík, P., Microstructure characterization of two Si_3N_4 based nanocomposites. In Proceedings of Deformation and Fracture in Structural PM Materials, ed. L. Parilák, and H. Danninger, Stará Lesná, Vol. 2, September 2002, pp. 82–86.
16. Morrell, R., *Handbook of Properties of Technical and Engineering Ceramics: An Introduction for the Engineer and Designer*. HMSO, London, 1985.